EUROPEAN ORGANIZATION FOR NUCLEAR RESEARCH

CERN/EP 84-81
9 July 1984

INCLUSIVE K^0_s, Λ AND $\bar{\Lambda}$ PRODUCTION IN 360 GEV/C pp INTERACTIONS USING THE EUROPEAN HYBRID SPECTROMETER

EHS-RCBC Collaboration

Bombay[1], CERN[2], Genova[3], Innsbruck[4], Japan-UG[5], Madrid[6], Mons[7], Rutgers[8], Serpukhov[9], Tennessee[10], Vienna[11] Collaboration

M. Asai[5(d)], J.L. Bailly[7], S. Banerjee[1], F. Bruyant[2], W.M. Bugg[10], C. Caso[2], H. Dibon[11], R. Di Marco[8], T. Emura[5(b)], B. Epp[4], A. Ferrando[6], Y. Fisyak[9], F. Fontanelli[3], P. Girtler[4], A. Gurtu[1], R. Hamatsu[5(a)], E.L. Hart[10], P. Herquet[7], J. Hrubec[11], Y. Iga[5a], N. Khalatjan[9(+)], E. Kistenev[9], P. Ladron de Guevara[6], J. MacNaughton[11], J.C. Marin[2], L. Montanet[2], G. Neuhofer[2], N. Ohshima[5(a)], Y. Petrovikh[9], P. Porth[11], B. Pijlgroms[2], M. Regler[11], T. Rodrigo[6], J. Salicio[6], S. Squarcia[3], P. Stamer[8], V. Stopchenko[9], U. Trevisan[3], C. Willmott[6] and G. Zholobov[9].

1 Tata Institute of Fundamental Research, Bombay, India
2 CERN, European Organization for Nuclear Research, Geneva, Switzerland
3 University of Genova and INFN, Genova, Italy
4 Inst. für Experimentalphysik, Innsbruck, Austria(++)
5(a) Tokyo Metropolitan University, Tokyo, Japan
(b) Tokyo University of Agriculture and Technology, Tokyo, Japan
(c) Chuo University, Tokyo, Japan
(d) Hiroshima University, Hiroshima, Japan
6 Junta de Energia Nuclear, Madrid, Spain
7 Université de l'Etat, Faculté des Sciences, Mons, Belgium
8 Rutgers University, New Brunswick, USA
9 Inst. for High Energy Physics, Serpukhov, USSR
10 University of Tennessee, Knoxville, USA
11 Inst. für Hochenergiephysik, Vienna, Austria(++)

Submitted to Zeitschrift für Physik C

(+) Also at Erevan Phys. Institute, Armenian Acad. Science, USSR
(++) Supported by Fonds zur Förderung der Wissensch. Forschung.

EP/2107P/CC/sb

ABSTRACT

Results on cross sections, longitudinal and transverse momentum distributions for K^o_s, Λ and $\bar{\Lambda}$ production in 360 GeV/c pp interactions are presented as obtained from EHS equipped with the Rapid Cycling Bubble Chamber (RCBC). The Λ and $\bar{\Lambda}$ polarizations are measured. The cross section for the diffractive components is given using the recoil spectrum. The data are discussed with respect to charm production.

1. INTRODUCTION

Strange particle production from proton-proton interactions at high energies is of considerable interest in the context of heavy flavour production in the quark-parton picture. Gustafson and Peterson [1] have argued that the amplitudes squared for diffraction dissociation into pions only, strangeness and charm are related as $2/m_{u,d}^2 : 1/m_s^2 : 1/m_c^2$ times a Regge factor accounting for the appropriate thresholds. With the introduction of flavour excitation models [2,3], heavy quark-antiquark production has become more complicated and has not yet been applied to the experimental data of strange particle production.

The observation of strange particle production in proton-proton interaction has been reported for various incident energies [4-14], and shows the general following characteristics: whereas both the K^o and $\bar{\Lambda}$ production increase rapidly with increasing energy, and occur predominantly in the central region, the Λ production is only slowly increasing and has a large contribution from the fragmentation processes.

In this article, we present a new determination of the strange particle inclusive cross sections and an attempt to separate the diffractive dissociation contribution. We also present results on the polarization of the Λ and $\bar{\Lambda}$. We finally compare our results to the charm production cross section observed at the same energy.

2. EXPERIMENTAL PROCEDURE AND CROSS SECTIONS

This experiment (NA23) has been performed at CERN with the European Hybrid Spectrometer (EHS) equipped with the Rapid Cycling Bubble Chamber (RCBC) filled with liquid hydrogen, exposed to a beam of 360 GeV/c protons coming from the H2 beam line. The experimental set-up together with the triggering conditions are described in ref. [15].

The data used in this analysis are based on a sample of 8564 inelastic events containing at least one V^o. This sample which represents ~ 80% of a 160 K picture exposure corresponds to a sensitivity of ~ 1.3 events/μb.

The events were measured by automatic and/or manual devices; the measurements were processed through the CERN hybrid geometry program GEOHYB and then a kinematics program tried to fit 3C V^o's and γ's to the production vertex. A check of the compatibility of the measurements obtained by the different machines was performed.

In what follows only unique 3C-fits events will be considered and to correct for ambiguities among different hypotheses the V^o decay angular distributions were studied. In fact, a simple kinematical calculation shows that ambiguities are expected to occur in well defined regions of the relevant angular distributions. For example, nearly all K^o/Λ, $K^o/\bar{\Lambda}$ and K^o/γ ambiguities are expected to be located in the regions $|\cos\theta^*| \geq 0.8$, where θ^* is the decay angle in the strange particle c.m.s.

In fig. 1 we show the decay angular distributions for unique fits. We observe for example that nearly all the forward Λ region ($\cos\theta^* > 0.$) is dominated by the K^o/Λ ambiguity. These angular distributions justify the following cuts applied to extract from the unique events the inclusive cross sections:

- Only K^o's with $|\cos\theta^*| \leq 0.8$ are accepted, and the cross sections are corrected accordingly ($w_{K^o} = 1.25$);

- Only Λ's with $-1.0 \leq \cos\theta^* \leq 0.$ are accepted and a correction factor $w_\Lambda = 2.0$ is applied.

- Only $\bar{\Lambda}$'s with $-.90 \leq \cos\theta \leq -.55$ and $.05 \leq \cos\theta^* \leq .95$ are accepted, with a correction factor $w_{\bar{\Lambda}} = 1.6$.

In addition to these correction factors, we have applied some further cuts to improve the quality of the data:

(a) We remove all V^o having at least one charged track badly measured ($\Delta p/p > 20\%$);

(b) We accept an hypothesis as unique if:

- its kinematical solution has a probability $\geq 2\%$,
- all competitive solutions have a probability $< 10^{-4}$.

Each event was individually weighted to correct for the probability to decay outside a fiducial volume or too close to the production vertex.

This momentum dependent weighting factor is

$$\left[e^{-\frac{\ell_o}{\bar{\ell}}} - e^{-\frac{\ell}{\bar{\ell}}} \right]^{-1}$$

where $\bar{\ell} = \beta\gamma c\tau$; $\ell_o = \ell_{min}/\cos\lambda$ and ℓ = potential length. We have found ℓ_{min} = 3.0 cm for all particles and all momenta. The interaction probability was properly taken into account using a rough parametrization of the K^o, Λ and $\bar{\Lambda}$ cross section momentum dependence. We corrected for scanning efficiencies and for the different losses during the various stages of the processing (measurements, geometry and kinematics inefficiencies).

Finally, we took advantage of the symmetry of a pp system to avoid the losses of strange particles decaying in the spectrometer. In fact, we restricted to particles produced in the backward hemisphere, which are mainly detected by the bubble chamber alone. With all the weights and correction procedures described above, we obtained for the inclusive production cross sections, corrected for unseen decay modes

$$\sigma(pp \to K^o_s X) = (8.55 \pm 0.51) \text{ mb},$$

$$\sigma(pp \to \Lambda X) = (4.08 \pm 0.40) \text{ mb},$$

$$\sigma(pp \to \bar{\Lambda} X) = (0.43 \pm 0.12) \text{ mb},$$

where the errors include statistical and systematic effects.

Figs 2 and 3 show a compilation of the cross sections as observed in proton-proton reactions. Our results agree with the existing information. The corresponding average number of strange particle per interaction are $\langle K^o_s \rangle = 0.26 \pm 0.01$, $\langle \Lambda \rangle = 0.12 \pm 0.02$ and $\langle \bar{\Lambda} \rangle = 0.013 \pm 0.004$, using $\sigma_{inel}(pp) = 32.80 \pm 0.50$ mb [15]. The topological cross sections are given in fig. 4 and table 1. The maximum of K^o_s production coincides with the one for charged multiplicity distribution ($n_{CH} = 8$), while for Λ and $\bar{\Lambda}$ it is situated at $n_{CH} = 10$. The associated average numbers of K^o_s, Λ and $\bar{\Lambda}$ are

also given in table 1. They show linear relations which can be parametrized in terms of $\langle V^o \rangle_{n_-} = \alpha + \beta n_-$, where n_- is the number of negative particles.

We have determined, for $n_- < 4$, the following values of α and β:

$$K^o_s \begin{cases} \alpha = 0.128 \pm 0.010, \\ \beta = 0.061 \pm 0.013. \end{cases}$$

$$\Lambda \begin{cases} \alpha = 0.051 \pm 0.013, \\ \beta = 0.030 \pm 0.009. \end{cases}$$

$$\bar{\Lambda} \begin{cases} \alpha = 0.0036 \pm 0.0063, \\ \beta = 0.0040 \pm 0.0050. \end{cases}$$

From the above parameters we can deduce that at our energy $\langle K^o_s \rangle_{n_-}/\langle K^o_s \rangle = (0.49 \pm 0.03) + (0.23 \pm 0.05)n_-$, $\langle \Lambda \rangle_{n_-}/\langle \Lambda \rangle = (0.43 \pm 0.14) + (0.25 \pm 0.09)n_-$ and $\langle \bar{\Lambda} \rangle_{n_-}/\langle \bar{\Lambda} \rangle = (0.28 \pm 0.50) + (0.31 \pm 0.40)n_-$; it follows that $\sigma_n(V^o)/\langle V^o \rangle = (0.40 + 0.26\ n_-)\sigma_n$ which is very similar to the value found at 405 GeV/c [11].

3. DIFFRACTIVE PRODUCTION

Fig. 5 shows the x-distribution of the fastest positive particle, assumed to be a proton. As expected, an accumulation is visible for $x > 0.85$, corresponding to the target diffraction. To estimate the background under the diffractive peak, the x-distribution was fitted in the range $0.2 \leq x \leq 0.85$ to the form $(1-x)^n$, with $n = 0.88 \pm 0.15$ for K^o_s and $\bar{\Lambda}$ events and $n = 1.29 \pm 0.39$ for Λ events separately. The extrapolation of this functions to $x > 0.85$ yields a contribution of $\sim 29.4\%$ for the background under the diffractive peak for K^o_s and $\bar{\Lambda}$ events, and $\sim 14.9\%$ for Λ. In addition, a correction of $\sim 6.3\%$ is introduced to account for the diffractive events with a K^o_s in the forward region. Finally, taking into account the spectrometer inefficiency at $x \sim 1$ ($\sim 12\%$), we obtained the following values:

$$\sigma\ ((pp)_{\text{"diff"}} \rightarrow K^o_s X) = (0.40 \pm 0.06)\ \text{mb},$$

$$\sigma\ ((pp)_{\text{"diff"}} \rightarrow \Lambda X) = (0.18 \pm 0.05)\ \text{mb},$$

$$\sigma\ ((pp)_{\text{"diff"}} \rightarrow \bar{\Lambda} X) = (0.017 \pm 0.012)\ \text{mb}.$$

These diffractive cross sections represent ~ 5% of the corresponding inclusive ones.

4. INVARIANT CROSS SECTIONS FOR K^o_s, Λ and $\bar{\Lambda}$ PRODUCTION

To study differential cross sections, we have introduced a momentum dependent weight for each observed unique decay. This procedure is illustrated in fig. 6 which shows the distribution of the transverse momentum of a V^o decay product as function of α

$$\alpha = \frac{p_L^+ - p_L^-}{p_L^+ + p_L^-} ,$$

(where $p_L^{\pm}$ is the laboratory longitudinal momentum of the positive (negative) particle of the V^o decay) for K^o, Λ and $\bar{\Lambda}$ all together. This picture clearly shows where the ambiguities are concentrated and the most relevant formulae to account for this ambiguity weight are given in refs [16,17].

The Feynman-x dependence of the invariant cross section of neutral strange particle production in high energy pp interactions may be interpreted by the presence of strange sea quarks in the central region for the K^o and by fragmentation mechanism for the Λ, which appears to have a maximum at $|x| \sim 0.5$ rather than a simple power behaviour in $(1-|x|)$. The $|x|$ distribution of Λ in the fragmentation region is a rather good test of the counting rules [18].

The invariant cross section for K^o_s production is shown in fig. 7. Our values are compared in the same figure to those obtained at 405 GeV/c [11]. The behaviour of the inclusive spectrum is compared to various theoretical predictions [18]. The results are given in table 2. Although the quark-exchange picture (drawn in fig. 7) seems to be favoured, we cannot rule out the other predictions. Furthermore, the shape of the distribution appears rather unaffected when we select the diffractive events. This result is consistent with factorisation as a dominant feature in diffraction dissociation.

The K^o_s differential cross section as a function of p_T^2 (fig. 8) shows a break at around 0.3 $(GeV/c)^2$. A fit to a double-slope form $e^{-bp_T^2}$ gives a good description of the data. The values found are
$b = 5.28 \pm 0.62\ (GeV/c)^{-2}$ for $0. \leq p_T^2 < 0.3\ (GeV/c)^2$ and
$b = 3.69 \pm 0.34\ (GeV/c)^{-2}$ for $0.3 \leq p_T^2 < 1.5\ (GeV/c)^2$. Comparable results were found at 405 GeV/c [11]. The double slope form is expected as due to the decay effect of K^*'s of high mass.

The invariant cross section for Λ production is shown in fig. 9 together with the values obtained at 405 GeV/c [11]. The best description of the data in the fragmentation region ($|x| \geq 0.5$) is obtained using the $(1-x)^1$ dependence (the fit of the data to the form $(1-x)^b$ in that range of $|x|$ gives $b = 1.22 \pm 0.25$, in very good agreement with the quark-exchange model [18]). The fusion quark-diquark model [19] predicts a form $F(x) \sim x^{b_1}\ (1-x)^{b_2}$ for the fragmentation region with $b_1 = 1.2$ for a spin 0 diquark and 2 for spin 1 and, in both cases, $b_2 = 1$. The data fits $b_1 = 1.13 \pm 0.37$ and $b_2 = 1.59 \pm 0.23$. Within two standard deviations our data are in agreement with the production of Λ through a spin 0 valence diquark.

The $d\sigma/dp_T^2$ distribution of the Λ (fig. 10) shows a clear break at around 0.6 $(GeV/c)^2$. A fit to a double-slope form $e^{-bp_T^2}$ gives
$b = 4.40 \pm 0.70\ (GeV/c)^{-2}$ for $0.1 \leq p_T^2 < 0.6\ (GeV/c)^{-2}$ and
$b = 2.20 \pm 0.66\ (GeV/c)^{-2}$ for $0.6 \leq p_T^2 < 1.5\ (GeV/c)^{-2}$.

The break in the $d\sigma/dt'$ (fig. 11) at $t' \sim 1.5\ (GeV/c)^2$ indicates that Λ production proceeds via two different mechanisms. The slopes are
$b_1 = 1.21 \pm 0.10\ (GeV/c)^{-2}$ for $0 \leq t' < 1.5\ (GeV/c)^2$ and
$b_2 = 0.51 \pm 0.16\ (GeV/c)^{-2}$ for $1.5 \leq t' < 6.0\ (GeV/c)^2$. In fact, the contribution to $d\sigma/dt'$ of both the fragmentation production ($|x| \geq 0.5$) and the central production ($|x| < 0.5$) is clearly differentiated in fig. 12.

The invariant cross section for $\bar{\Lambda}$ production is shown in fig. 13 and is compared to a $(1 - x)^5$ distribution. It shows agreement with the

gluon exchange model and point-like pair creation [18]. The $d\sigma/dt'$ spectrum (not shown) behaves as $e^{-(0.42 \pm 0.14)t'}$ comparable in slope with the one for K^o_s, revealing an essentially central production.

5. Λ AND $\bar{\Lambda}$ POLARIZATION

The Λ and $\bar{\Lambda}$ polarization has been determined using the distribution

$$\frac{dN}{d\cos\theta} = \frac{1}{2}(1 + \alpha P_\Lambda \cos\theta),$$

where θ is the angle between the unit vector $\hat{n} = (\vec{p}_p \times \vec{p}_\Lambda)/|\vec{p}_p \times \vec{p}_\Lambda|$ and daughter proton, and $\alpha = 0.642 \pm 0.013$. For both Λ and $\bar{\Lambda}$ we have taken $\vec{p}_p$ to be the target proton and α has been taken with a negative sign for $\bar{\Lambda}$. The average polarizations of Λ and $\bar{\Lambda}$ have been found to be

$$P_\Lambda = -0.24 \pm 0.09; \quad P_{\bar{\Lambda}} = +0.36 \pm 0.35.$$

The Λ polarization is shown as a function of x_Λ in fig. 14 along with similar measurements done in 6 and 19 GeV/c pp experiments [20]. All the polarization data seem to have similar characteristics namely large positive polarization at large $|x_\Lambda|$ values which go to small values (zeroish) as x_Λ approaches zero. On the same figure predictions from the quark model of DeGrand and Miettinen [21] are shown. The large positive polarization at large $|x_\Lambda|$ values cannot be accounted for in that picture. The Λ polarization has been plotted as a function of Λ-transverse momentum in fig. 15 along with similar measurements in pp experiments [22] at 24 GeV/c and two ISR energies. Here one sees that the polarization is small at small p_T and that it is getting large negative values at large p_T. The predictions of quarks models à la DeGrand-Miettinen or Anderson et al. [23] are compatible with the trend observed in the data.

6. COMPARISON OF INCLUSIVE NEUTRAL STRANGE PARTICLE PRODUCTION WITH CHARM PARTICLE PRODUCTION

In order to compare charm to strangeness production in 360 GeV/c pp interactions, we have used the following results of ref. [24]

$$\sigma(D\bar{D}) = (19\ ^{+\ 13}_{-\ 5})\ \mu b \text{ and } \sigma(\Lambda_c \bar{D}) = (18\ ^{+\ 15}_{-\ 10})\ \mu b \text{ for all } x.$$

The ratio

$$\frac{\sigma(\Lambda_c \bar{D})}{\sigma(\Lambda)} = \frac{18\ ^{+\ 15}_{-\ 10}\ \mu b}{(4080 \pm 400)\mu b} = (4.4\ ^{+\ 3.7}_{-\ 2.5}) \times 10^{-3},$$

is of the order 1/200. This suppression factor applies to the proton fragmentation region and is characterized by $m_{\Lambda_c} + m_{\bar{D}} = 4.16$ GeV/c^2 as lowest charm production threshold.

An estimate of $\sigma(K\bar{K})$ can be extracted from $\sigma(K^o_s)$ and $\sigma(\Lambda)$, giving:

$$\frac{\sigma(D\bar{D})}{\sigma(K\bar{K})} = (1.3\ ^{+\ 0.9}_{-\ 0.4}) \times 10^{-3}\ .$$

This smaller suppression factor applies to central production. It is characterized by $m_D + m_{\bar{D}} + m_N = 4.68$ GeV/c^2 as lowest charm production threshold. Both charm/strangeness suppression factors are not inconsistent within the errors. The values of the $(c\bar{c}/s\bar{s})$ suppression factor obtained here may be compared with the value $(s\bar{s}/u\bar{u})$ of 0.29 ± 0.02 deduced by Malhotra and Orava [25]. Thus, the creation of charm quarks is considerably more suppressed as compared to the one for strange quarks.

7. SUMMARY OF THE RESULTS

- The inclusive cross sections for the production of neutral strange particles have been determined as:

  $\sigma(pp \to K^o_s X) = (8.55 \pm 0.51)$ mb,

  $\sigma(pp \to \Lambda X) = (4.08 \pm 0.40)$ mb,

  $\sigma(pp \to \bar{\Lambda} X) = (0.43 \pm 0.12)$ mb.

- The values for the inclusive topological cross sections for K^o_s, Λ and $\bar{\Lambda}$ production are given. It is found that $\sigma_n(V^o)/\langle V^o \rangle = (0.40 + 0.26\ n_-)\sigma_n$.

- The cross sections for proton diffraction dissociation into neutral strange particles have been determined as:

  $\sigma_D\ (pp \to pK^o_s X) = (0.40 \pm 0.06)$mb,

  $\sigma_D\ (pp \to p\Lambda X) = (0.18 \pm 0.05)$mb,

  $\sigma_D\ (pp \to p\bar{\Lambda} X) = (0.017 \pm 0.012)$mb.

- In the K^o_s structure function the central production is dominant. The Λ structure function shows a significant maximum at $|x| \sim 0.5$.

- The $|x|$ distribution of the K^o_s invariant cross section appears similar in shape for the whole sample and for the diffractive V^o events (the x of one positive particle is greater than 0.85). No relative shrinkage of the $|x|$ distribution is obtained.

- The Λ and $\bar{\Lambda}$ polarizations are determined as:

$$P_\Lambda = -0.24 \pm 0.09; \quad P_{\bar{\Lambda}} = 0.36 \pm 0.35.$$

- Using the charm production cross sections from 360 GeV/c pp interactions, obtained in EHS with experiment NA16, the following two charm/strangeness suppression factors have been obtained:

$$\sigma(\Lambda_c \bar{D})/\sigma(\Lambda) = (4.4 \, ^{+\,3.7}_{-\,2.5}) \times 10^{-3},$$

$$\sigma(D\bar{D})/\sigma(K\bar{K}) = (1.3 \, ^{+\,0.9}_{-\,0.4}) \times 10^{-3}.$$

REFERENCES

[1] G. Gustafson and C. Peterson, Phys. Letters 67B (1977) 81.

[2] V. Barger, F. Halzen and W.Y. Keung, Phys. Rev. D25 (1982) 112.

[3] R. Odorico, Nucl. Phys. B209 (1982) 77.

[4] K. Jaeger et al., 205 GeV/c pp, Phys. Rev. D11 (1975) 2405.

[5] G. Charlton et al., 205 GeV/c pp, Phys. Rev. Lett. 30 (1973) 574.

[6] F.T. Dao et al., 303 GeV/c pp, Phys. Rev. Lett. 30 (1973) 1151.

[7] A. Sheng et al., 300 GeV/c pp, Phys. Rev. D11 (1975) 1733.

[8] F. LoPinto et al., 300 GeV/c pp, Phys. Rev. D22 (1980) 573.

[9] R.D. Kass et al., 400 GeV/c pp, Phys. Rev. D20 (1979) 605.

[10] H. Kichimi et al., 405 GeV/c, Phys. Lett. 72B (1978) 411.

[11] H. Kichimi et al., 405 GeV/c pp, Phys. Rev. D20 (1979) 37.

[12] S. Erhan et al., $\sqrt{s}$ = 53 and 62 GeV, Phys. Lett. 85B (1979) 447.

[13] D. Drijard et al., $\sqrt{s}$ = 62 GeV, Zeitschr. für Phys. C12 (1982) 217.

[14] D. Drijard et al., $\sqrt{s}$ = 62 GeV, CERN/EP 83-5 (1983).

[15] J.L. Bailly et al., to be published in Zeitschr. für Phys. C Particles and Fields.

[16] R. Armenteros and J. Podolanski, Phil. Mag. 45 (1954) 13.

[17] C. Cochet et al., Nucl. Phys. B124 (1977) 61.

[18] S.J. Brodsky and J.F. Gunion, Phys. Rev, D17 (1978) 848;
J.F. Gunion, Phys. Lett. 88B (1979) 150.

[19] Yu. V. Fisjak and E.P. Kistenev, Zeitschr. für Phys. C. Particles and Fields 10 (1981) 307.

[20] A. Lesnik et al., Phys. Rev. Lett. 35 (1975) 710;
P. Aahlin et al., Lett. al Nuovo Cim. 21 (1978) 236.

[21] T.A. DeGrand, H.I. Miettinen, Phys. Rev. D23 (1981) 1227 and D24 (1981) 2419.

[22] V. Blöbel et al., Nucl. Phys. B122 (1977) 429;
S. Ehran et al., Phys. Lett. 22B (1979) 301.

REFERENCES (Cont'd)

[23] B. Anderson et al., Phys. Lett. 85B (1979) 417;
B. Anderson et al., LU-TP 82-13.

[24] M. Aguilar-Benitez et al., Phys. Letters 123B (1983) 103.

[25] P.K. Malhotra and R. Orava, Zeitschr. für Physik C Particles and Fields 17 (1983) 85.

TABLE CAPTIONS

Table 1 Topological cross sections for $pp \to (K^o_s, \Lambda, \bar{\Lambda}) + X$ and average number of K^o_s, Λ and $\bar{\Lambda}$ per inelastic collision.

Table 2 Fits to the $2E^*/\pi\sqrt{s}\, d\sigma/dx$ distributions for the K^o_s inclusive production.

TABLE 1

Topology	σ_n (pp) (mb)	$\sigma_n(K_s^0)$ (mb)	$\sigma_n(\Lambda)$ (mb)	$\sigma_n(\bar{\Lambda})$ (mb)	$\langle K_s^0 \rangle$	$\langle \Lambda \rangle$	$\langle \bar{\Lambda} \rangle$
2 (inel)	2.09 ± 0.36	0.26 ± 0.06	0.09 ± 0.05	-	0.12 ± 0.03	0.04 ± 0.02	-
4	4.40 ± 0.16	0.63 ± 0.10	0.45 ± 0.10	0.03 ± 0.02	0.14 ± 0.02	0.10 ± 0.02	0.008 ± 0.005
6	5.31 ± 0.18	1.24 ± 0.13	0.60 ± 0.12	0.07 ± 0.03	0.23 ± 0.03	0.11 ± 0.02	0.013 ± 0.006
8	5.95 ± 0.19	1.97 ± 0.17	0.72 ± 0.14	0.09 ± 0.03	0.33 ± 0.03	0.12 ± 0.02	0.015 ± 0.006
10	5.00 ± 0.17	1.86 ± 0.16	0.92 ± 0.15	0.10 ± 0.04	0.37 ± 0.03	0.18 ± 0.03	0.020 ± 0.008
12	4.05 ± 0.15	1.02 ± 0.12	0.56 ± 0.12		0.25 ± 0.03	0.14 ± 0.05	
> 10	10.05 ± 0.18			0.14 ± 0.10			0.014 ± 0.010
> 12	6.00 ± 0.09	1.57 ± 0.35	0.74 ± 0.31		0.26 ± 0.06	0.12 ± 0.05	
Total	32.80 ± 0.19	8.55 ± 0.51	4.08 ± 0.40	0.43 ± 0.12	0.26 ± 0.01	0.12 ± 0.02	0.013 ± 0.004

TABLE 2

From	Range of $\|x\|$	Parameters from fit [A(mb)]	χ^2/NDF	Prob.
(a) Quark-exchange or annihilation $A\,[(1-x)^3+2(1-x)^7]$	$0.05 \leq \|x\| < 0.525$	$A = 0.69 \pm 0.03$	7.0/10	72.4%
(b) Gluon exchange $A\,[(1-x)^5+(1-x)^9]$	$0.05 \leq \|x\| < 0.525$	$A = 1.26 \pm 0.06$	11.5/10	31.8%
(c) Gluon exchange + point-like pairs creation $A\,[(1-x)^4+(1-x)^5]$	$0.05 \leq \|x\| < 0.525$	$A = 0.92 \pm 0.04$	8.8/10	55.1%
(a) $A\,[(1-x)^{b_1}+2(1-x)^{b_2}]$	$0.05 \leq \|x\| < 0.525$	$A = 0.72 \pm 0.06$ $b_1 = 3.46 \pm 0.48$ $b_2 = 6.92 \pm 0.63$	6.3/8	61.4%
(b)+(c) $A\,[(1-x)^{b_1}+(1-x)^{b_2}]$	$0.05 \leq \|x\| < 0.525$	$A = 1.07 \pm 0.14$ $b_1 = 4.05 \pm 0.89$ $b_2 = 7.22 \pm 3.55$	6.4/8	60.7%

FIGURE CAPTIONS

Fig. 1 Distributions of the $\bar{\Lambda}$, Λ and K^o_s polar angles θ^* in their c.m.s.

Fig. 2 s dependence of the inclusive cross section for the reaction $pp \to K^o_s$ + anything.

Fig. 3 s dependence of the inclusive cross sections for the reactions $pp \to \Lambda$ + anything and $pp \to \bar{\Lambda}$ + anything.

Fig. 4 K^o_s, Λ and $\bar{\Lambda}$ topological cross sections. n_{ch} is the number of charged particles at production.

Fig. 5 Feynman-x distribution for the fastest positive secondary track with proton mass assignment.

Fig. 6 Armenteros-Podolanski plot of the neutral strange particle decays in the variable $\alpha = (p_L^+ - p_L^-)/(p_L^+ + p_L^-)$, where $p_L^\pm$ are the longitudinal momenta of the positive and negative decay products in the laboratory system with respect to the laboratory momentum of the decaying particle.

Fig. 7 Feynman-x distribution of the invariant cross section for fully inclusive and diffractive K^o_s production. The line corresponds to the function $(1-x)^3 + 2(1-x)^7$. Comparison is made to the distribution obtained at 405 GeV/c pp interactions [11].

Fig. 8 K^o_s inclusive production differential cross section as function of p_T^2.

Fig. 9 Feynman-x distribution of the invariant cross section for fully inclusive and diffractive Λ production. The line corresponds to the form $(1-x)^1$. Comparison is made to the distribution obtained at 405 GeV/c pp interactions [11].

FIGURE CAPTIONS (Cont'd)

Fig. 10 Λ inclusive production differential cross section as function of p_T^2.

Fig. 11 Λ inclusive production differential cross section as function of t' with $t' = |t-t_{min}|$.

Fig. 12 $d\sigma/dt'$ for Λ in the regions: $|x| < 0.5$ (•) and $|x| \geq 0.5$ (□).

Fig. 13 Feynman-x distribution of the invariant cross section for fully inclusive $\bar{\Lambda}$ production. The line corresponds to $(1-x)^5$.

Fig. 14 Dependence of the Λ polarization on x_Λ.

Fig. 15 Dependence of the Λ polarization on the Λ transverse momentum.

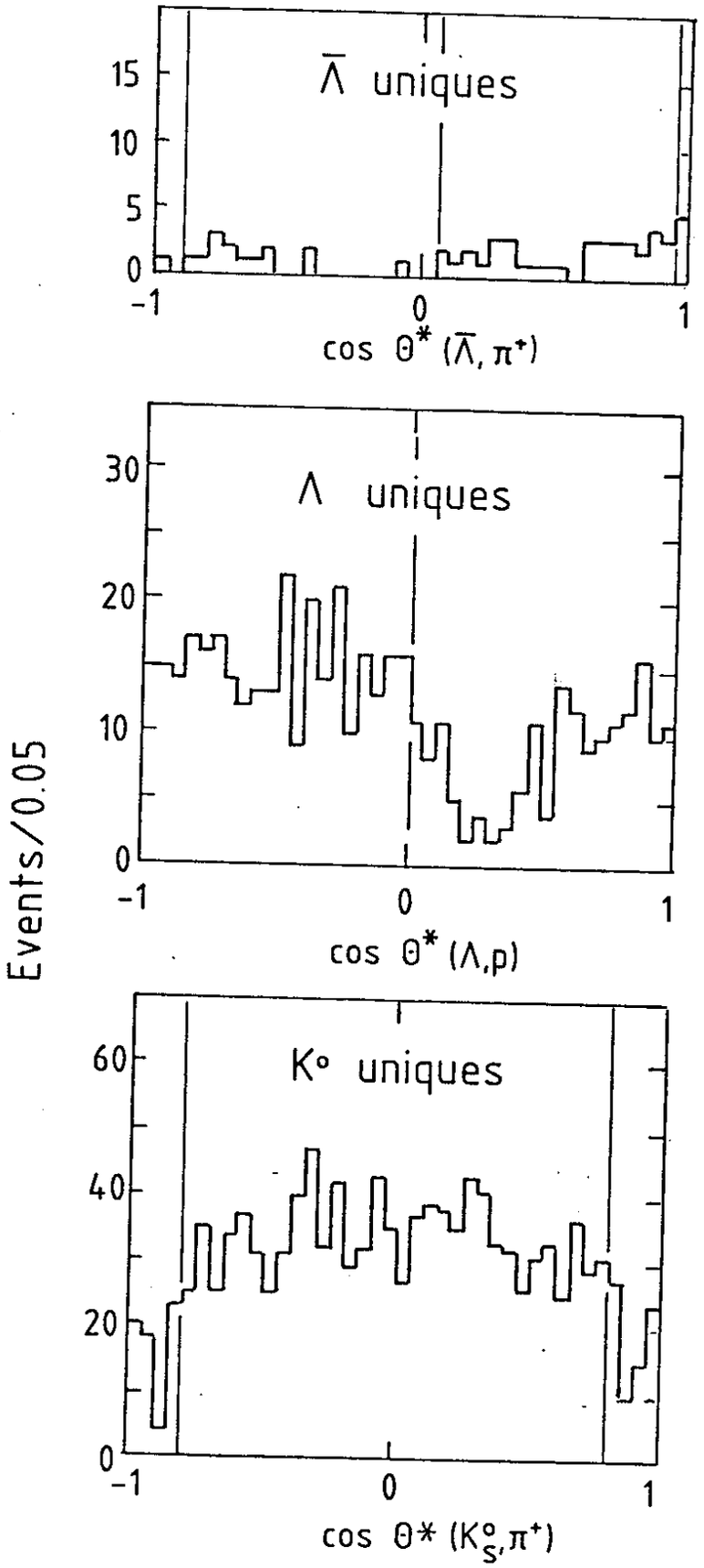
$\bar{\Lambda}$ uniques
15
10
5
0
-1
0
1
cos θ^* ($\bar{\Lambda}$, π^+)
Λ uniques
30
20
10
0
-1
0
1
cos θ^* (Λ,p)
Events/0.05
K° uniques
60
40
20
0
-1
0
1
cos θ^* (K^o_S,π^+)

Fig. 1

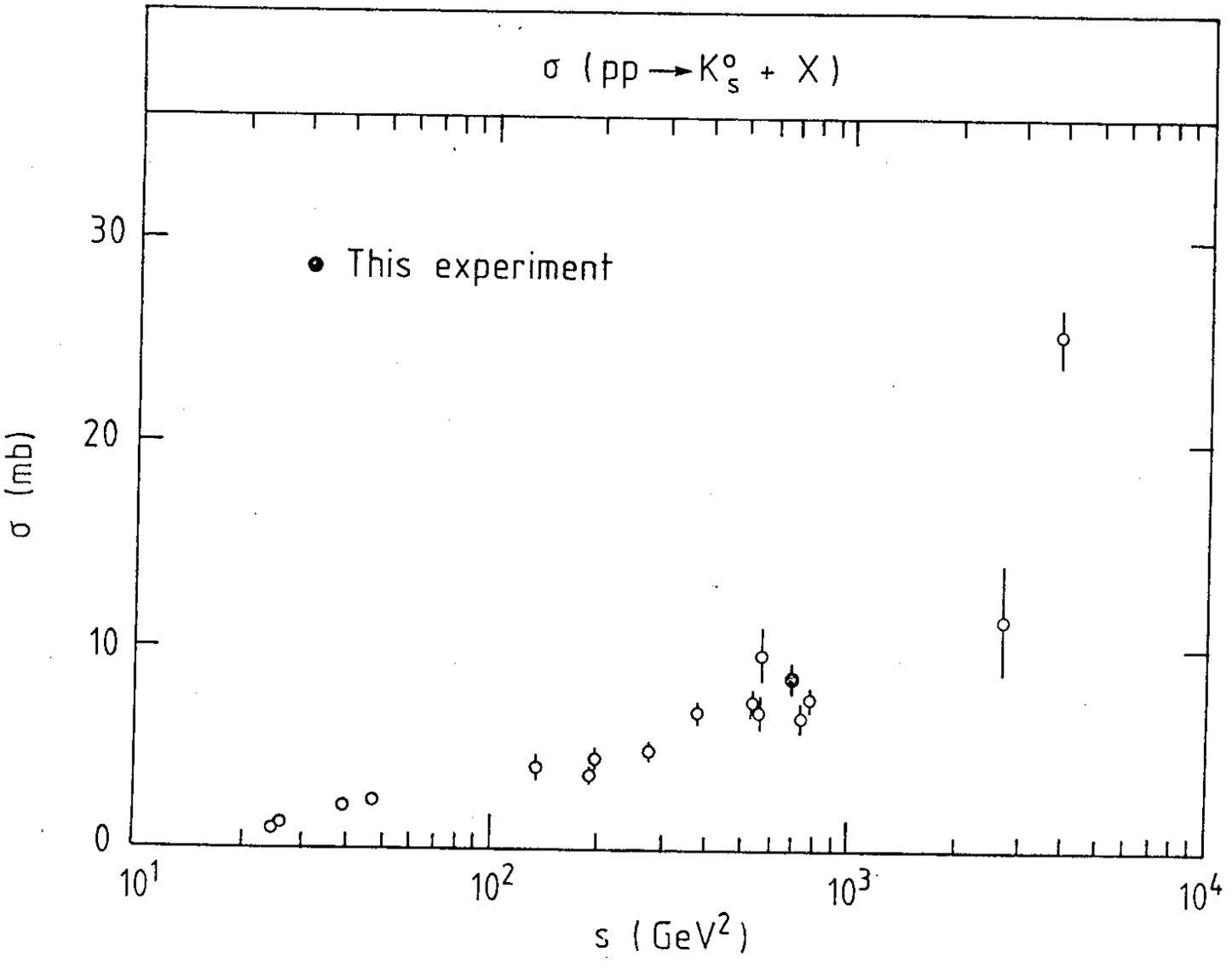

Fig. 2

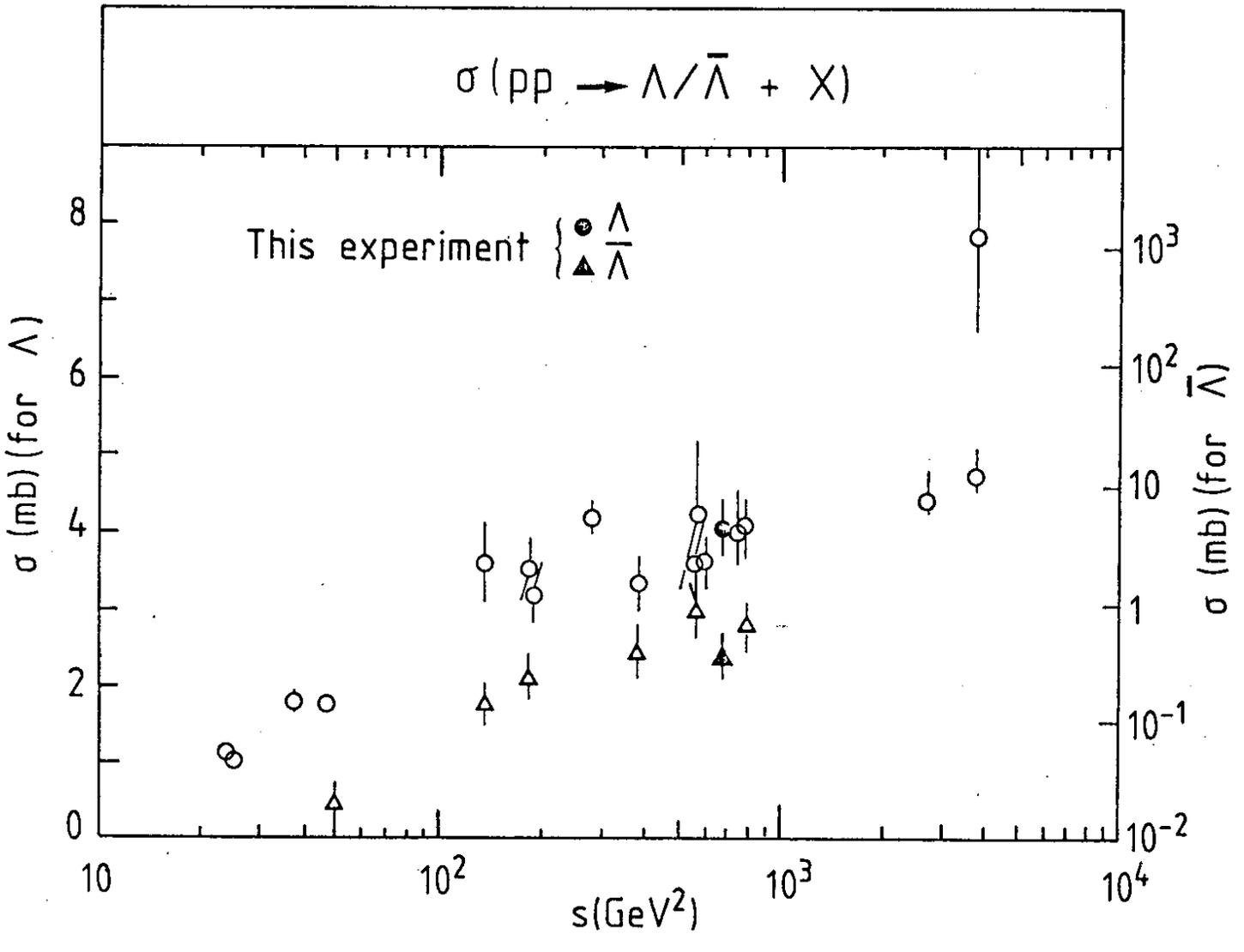
σ(pp → Λ/Λ̄ + X)
This experiment
Λ
Λ̄
σ (mb) (for Λ)
σ (mb) (for Λ̄)
s(GeV²)
0
2
4
6
8
10
10²
10³
10⁴
10⁻²
10⁻¹
1
10
10²
10³

Fig. 3

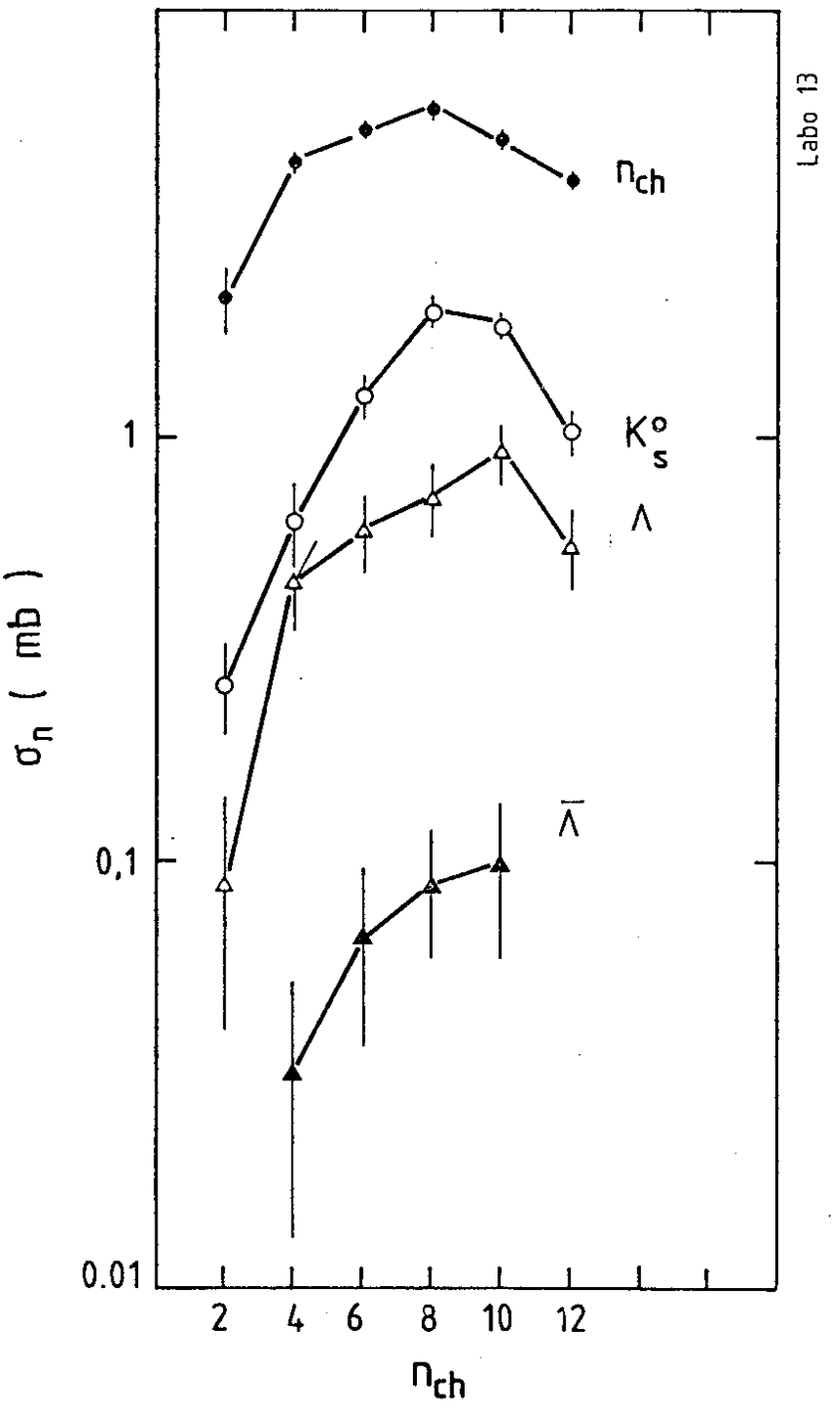
Labo 13
n_{ch}
K^o_s
Λ
$\bar{\Lambda}$
σ_n (mb)
1
0,1
0.01
2
4
6
8
10
12
n_{ch}

Fig. 4

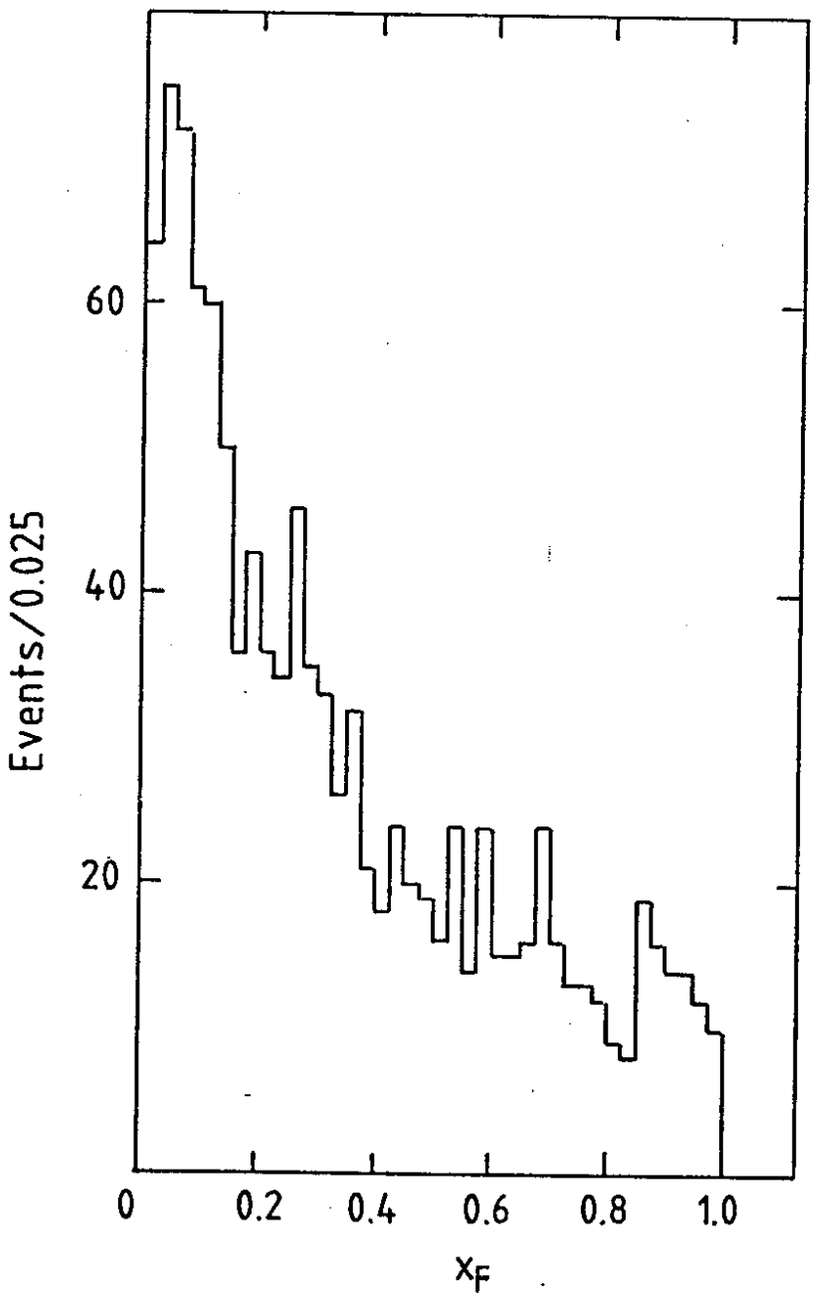

Fig. 5

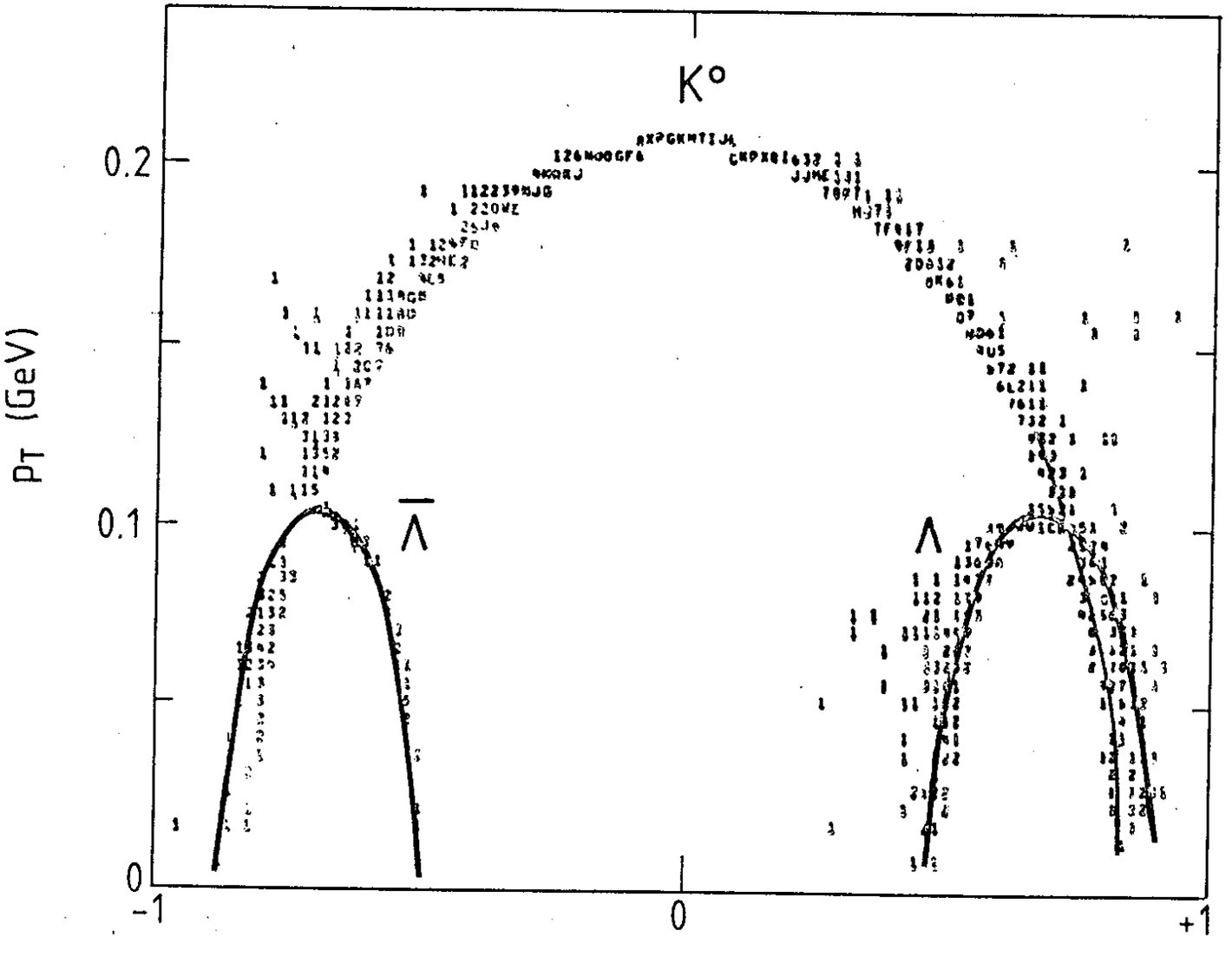

Fig. 6

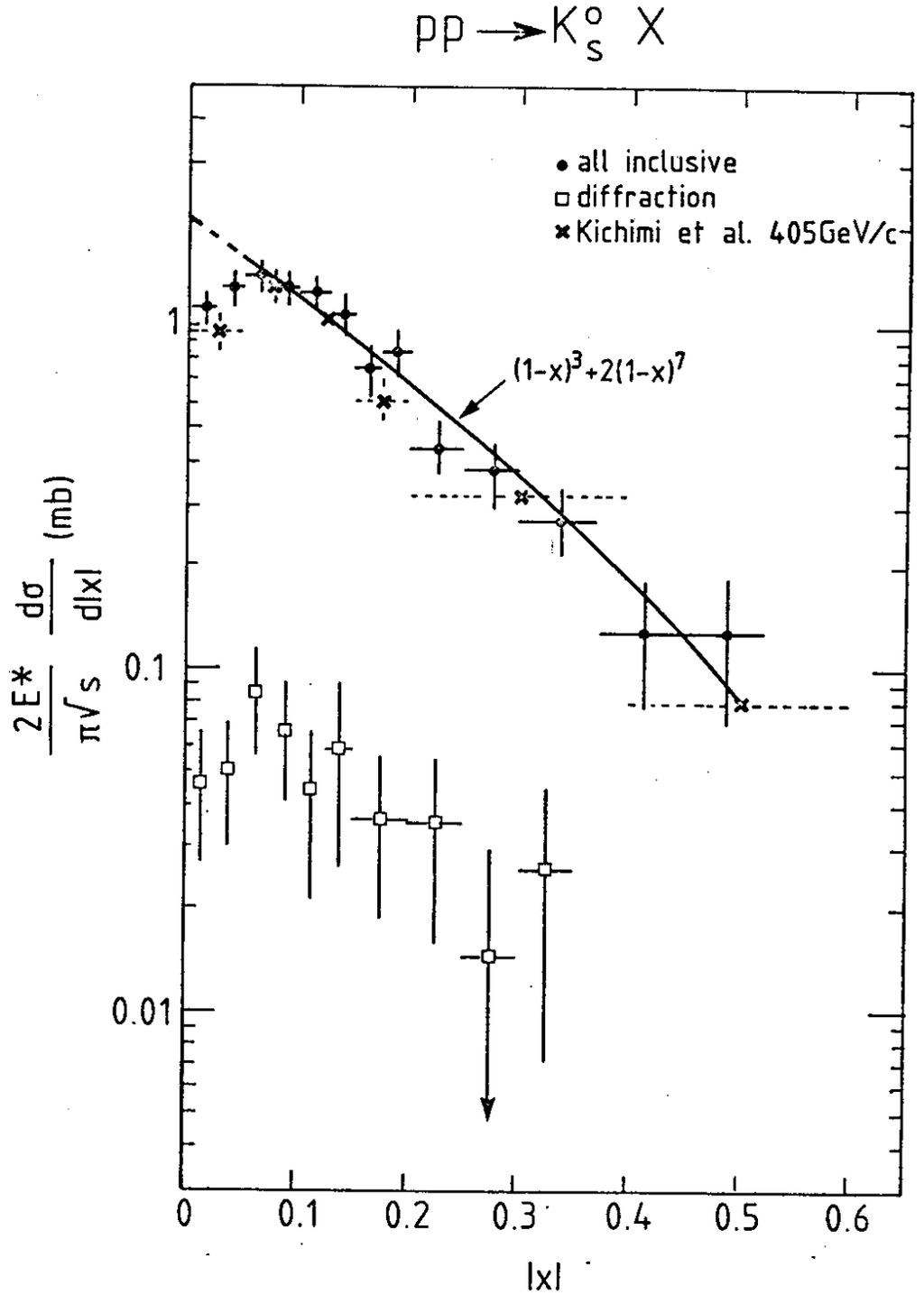
pp → K°s X
• all inclusive
□ diffraction
× Kichimi et al. 405GeV/c
(1-x)³+2(1-x)⁷
2E*/√s dσ/d|x| (mb)
1
0.1
0.01
0
0.1
0.2
0.3
0.4
0.5
0.6
|x|

Fig. 7

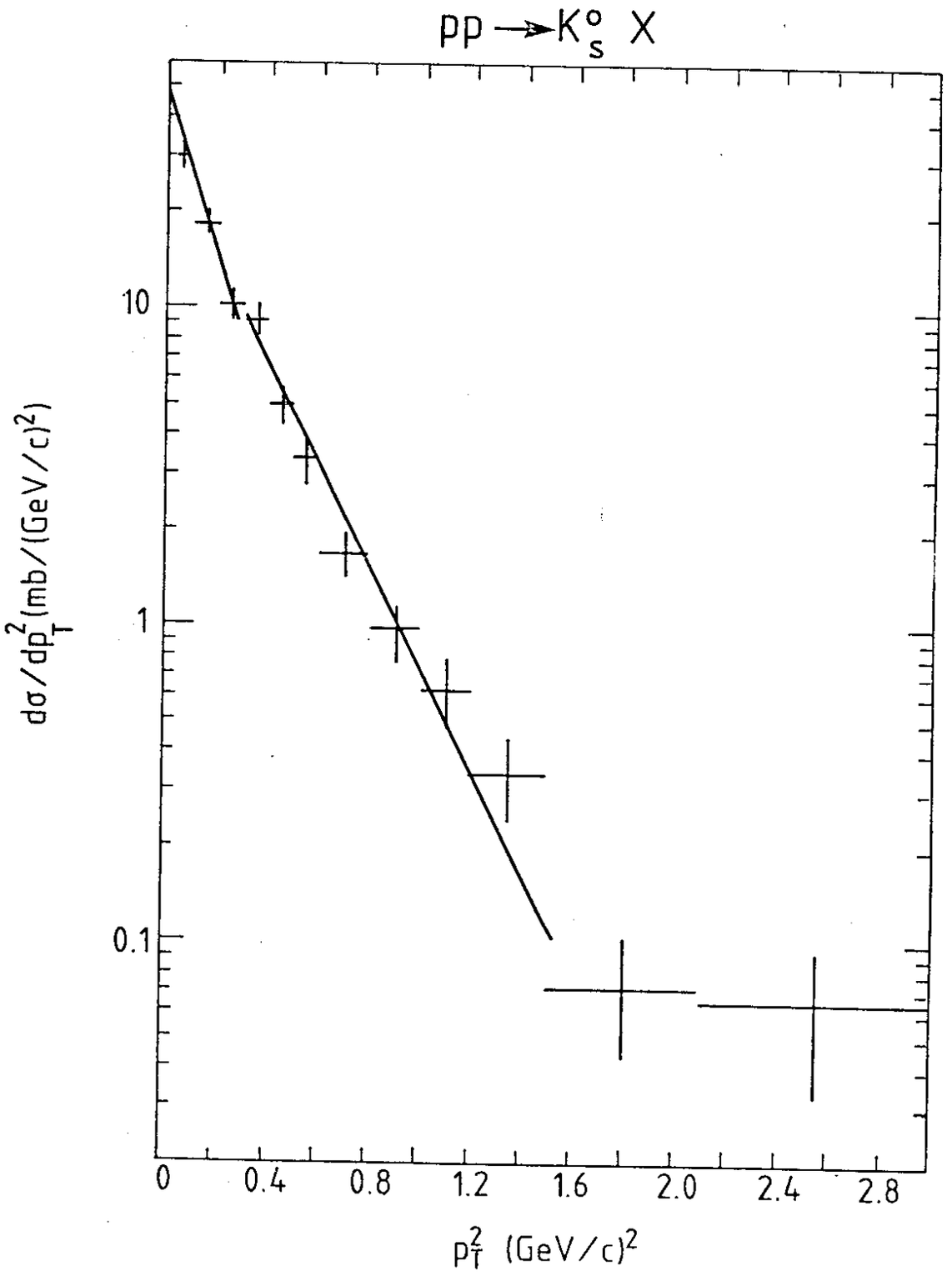

Fig. 8

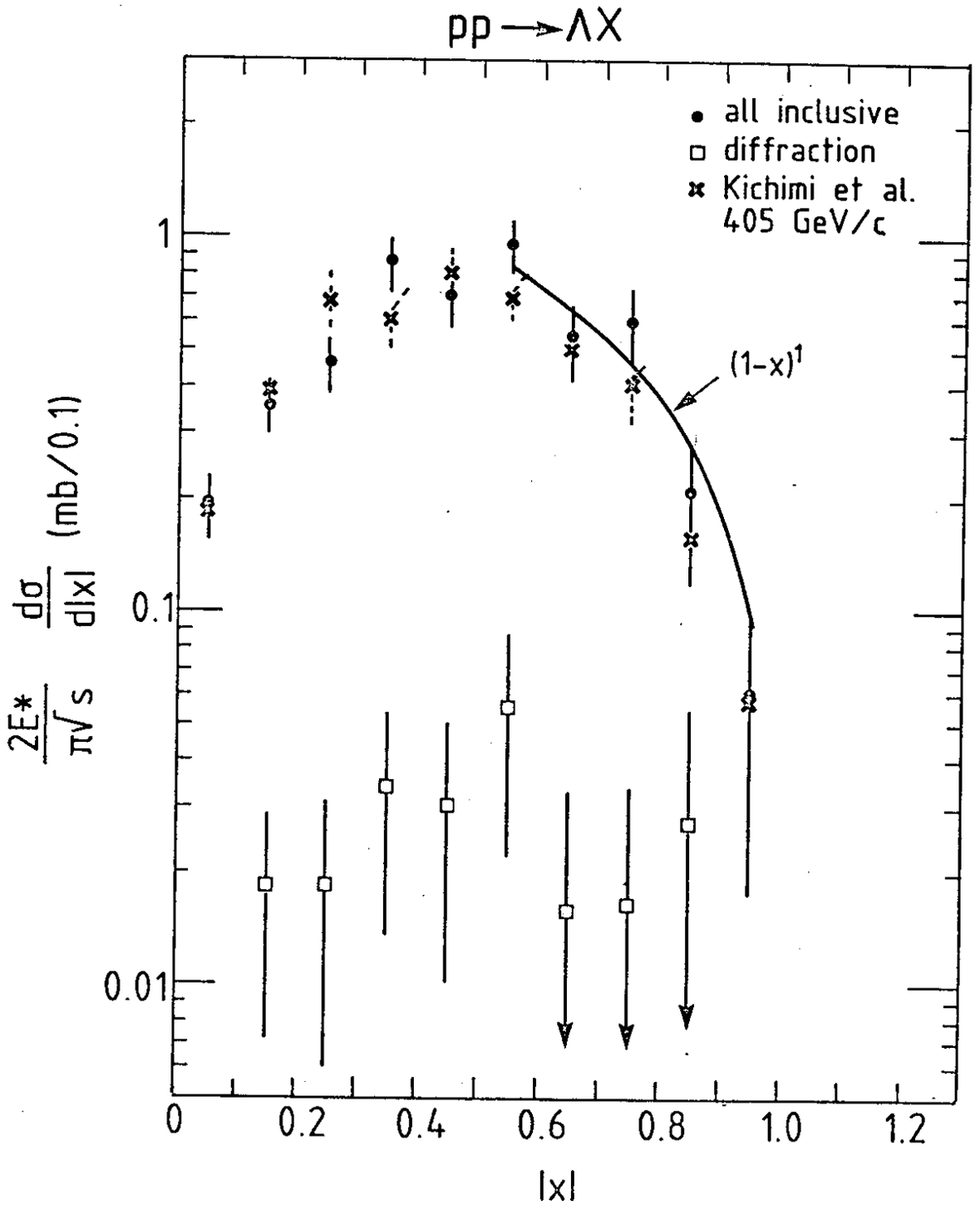
pp → ΛX
all inclusive
diffraction
Kichimi et al.
405 GeV/c
(1-x)¹
1
0.1
0.01
0
0.2
0.4
0.6
0.8
1.0
1.2
|x|
2E*/π√s dσ/d|x| (mb/0.1)

Fig. 9

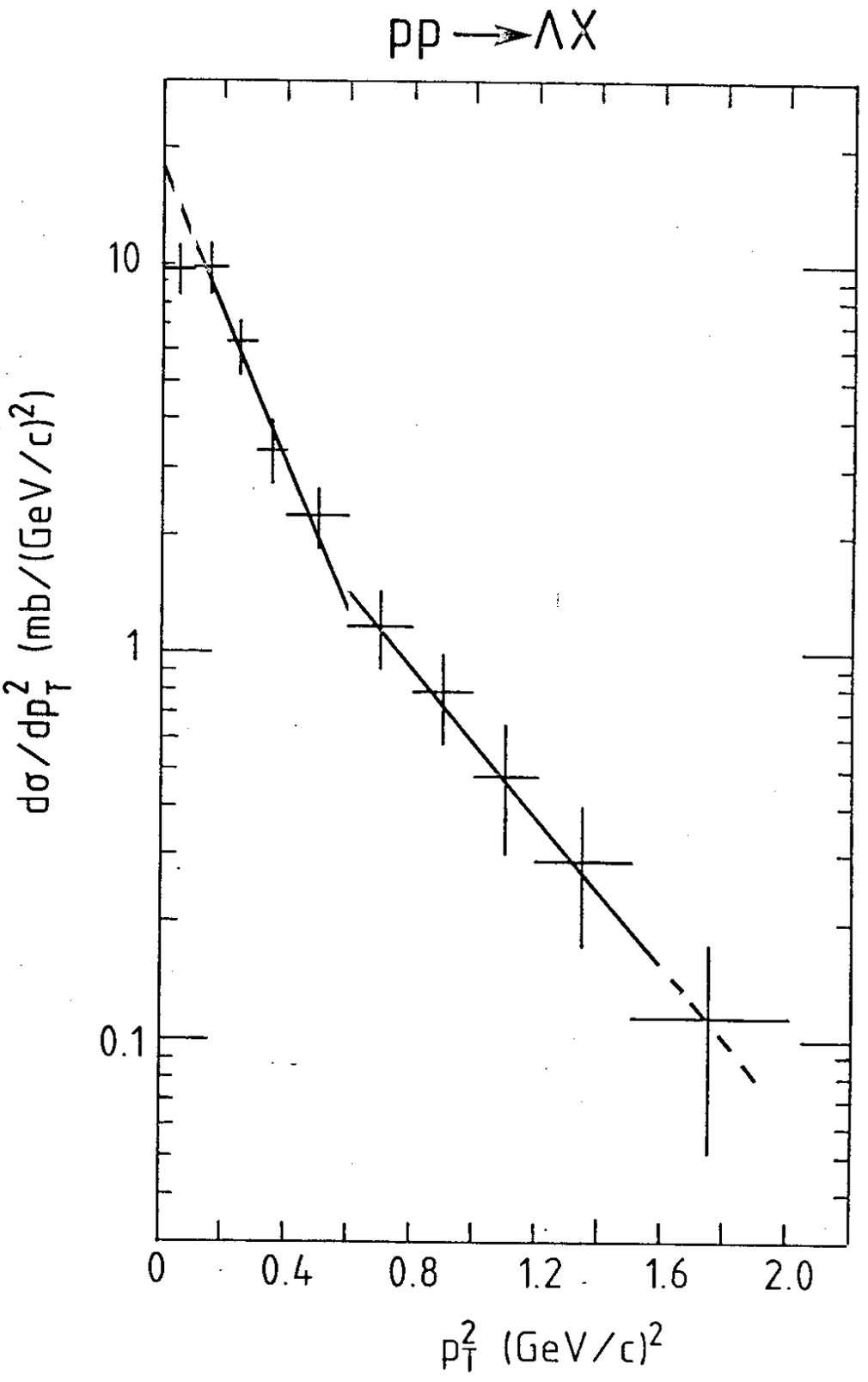

Fig. 10

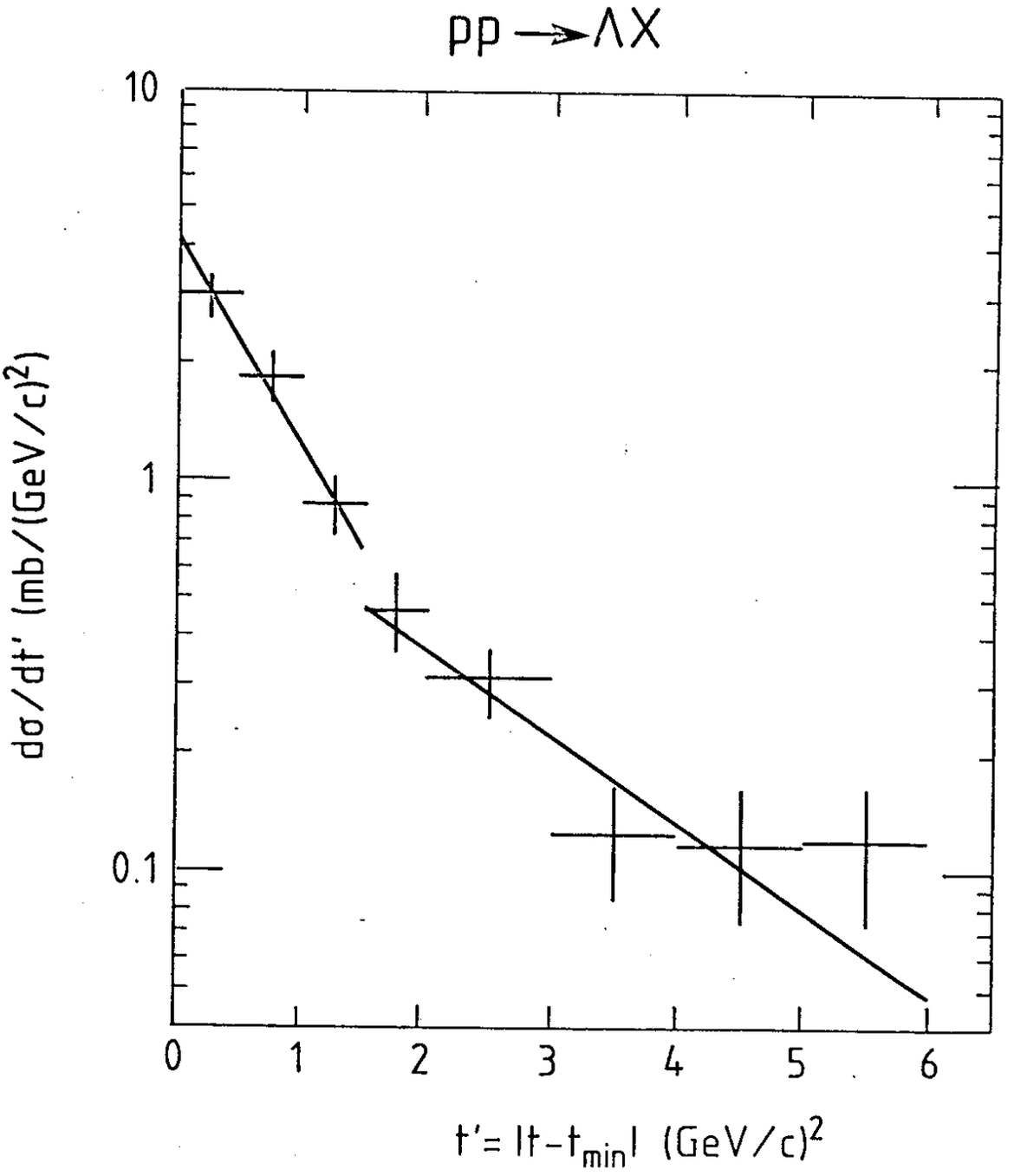

Fig. 11

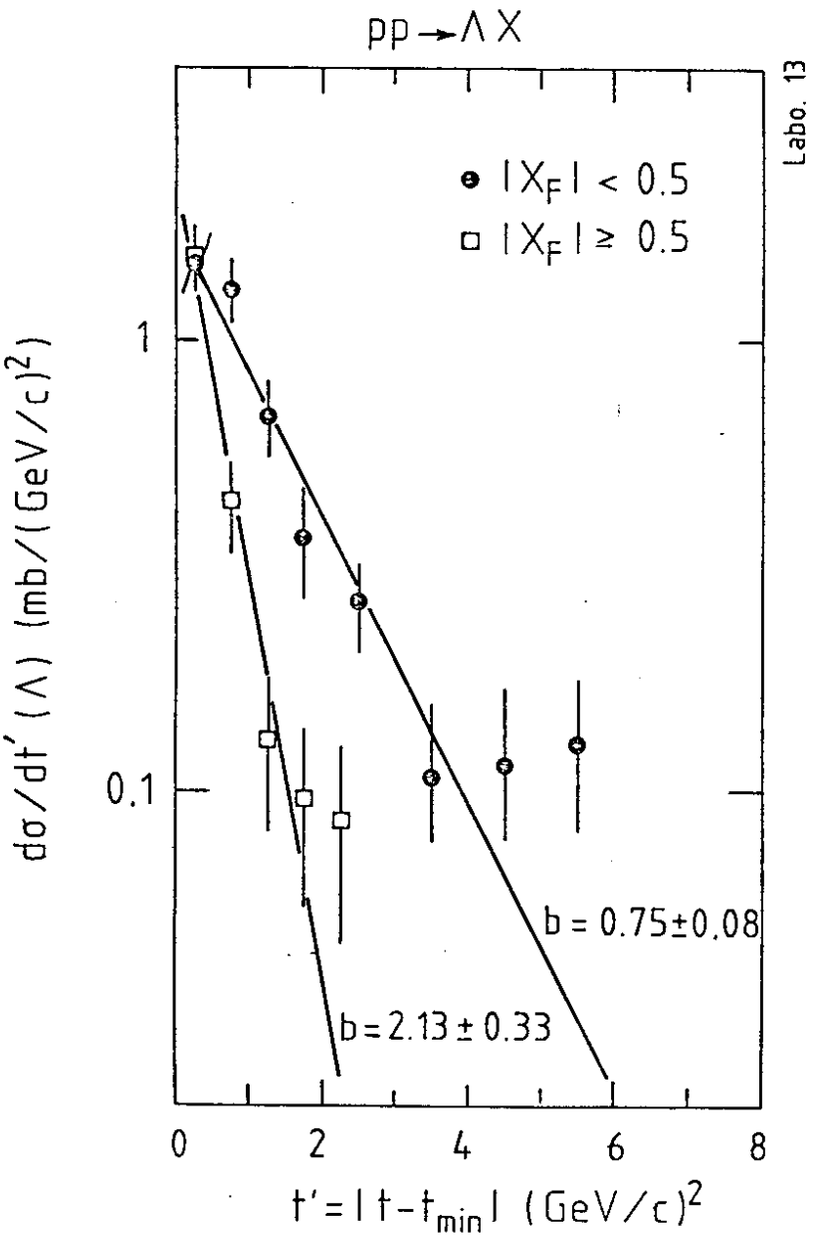
pp → Λ X
Labo. 13
● |X_F| < 0.5
□ |X_F| ≥ 0.5
1
0.1
dσ/dt' (Λ) (mb/(GeV/c)²)
b = 0.75±0.08
b = 2.13 ± 0.33
0
2
4
6
8
t' = |t-t_min| (GeV/c)²

Fig. 12

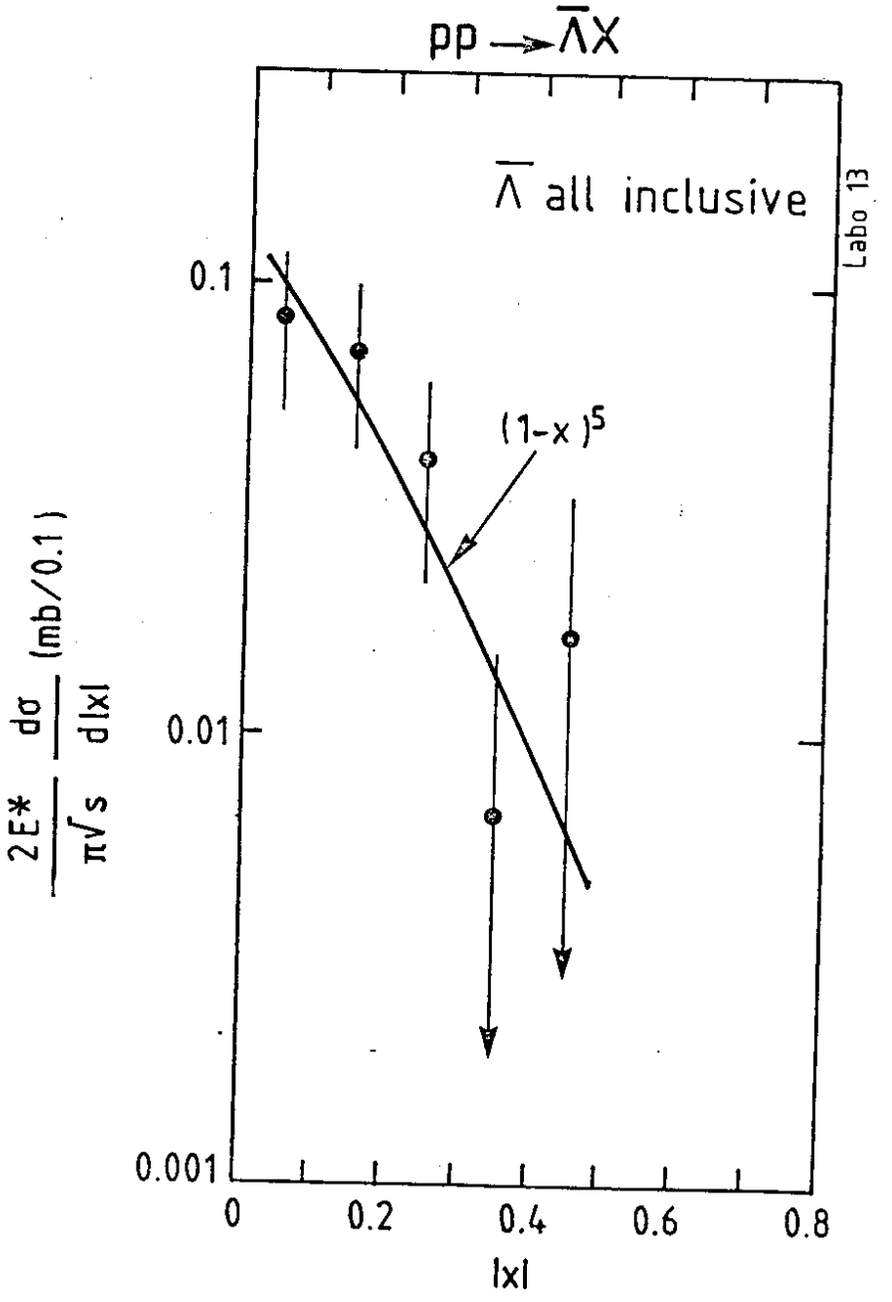
pp → Λ̄X
Λ̄ all inclusive
Labo 13
(1-x)^5
0.1
0.01
0.001
0
0.2
0.4
0.6
0.8
|x|
2E*/π√s dσ/d|x| (mb/0.1)

Fig. 13

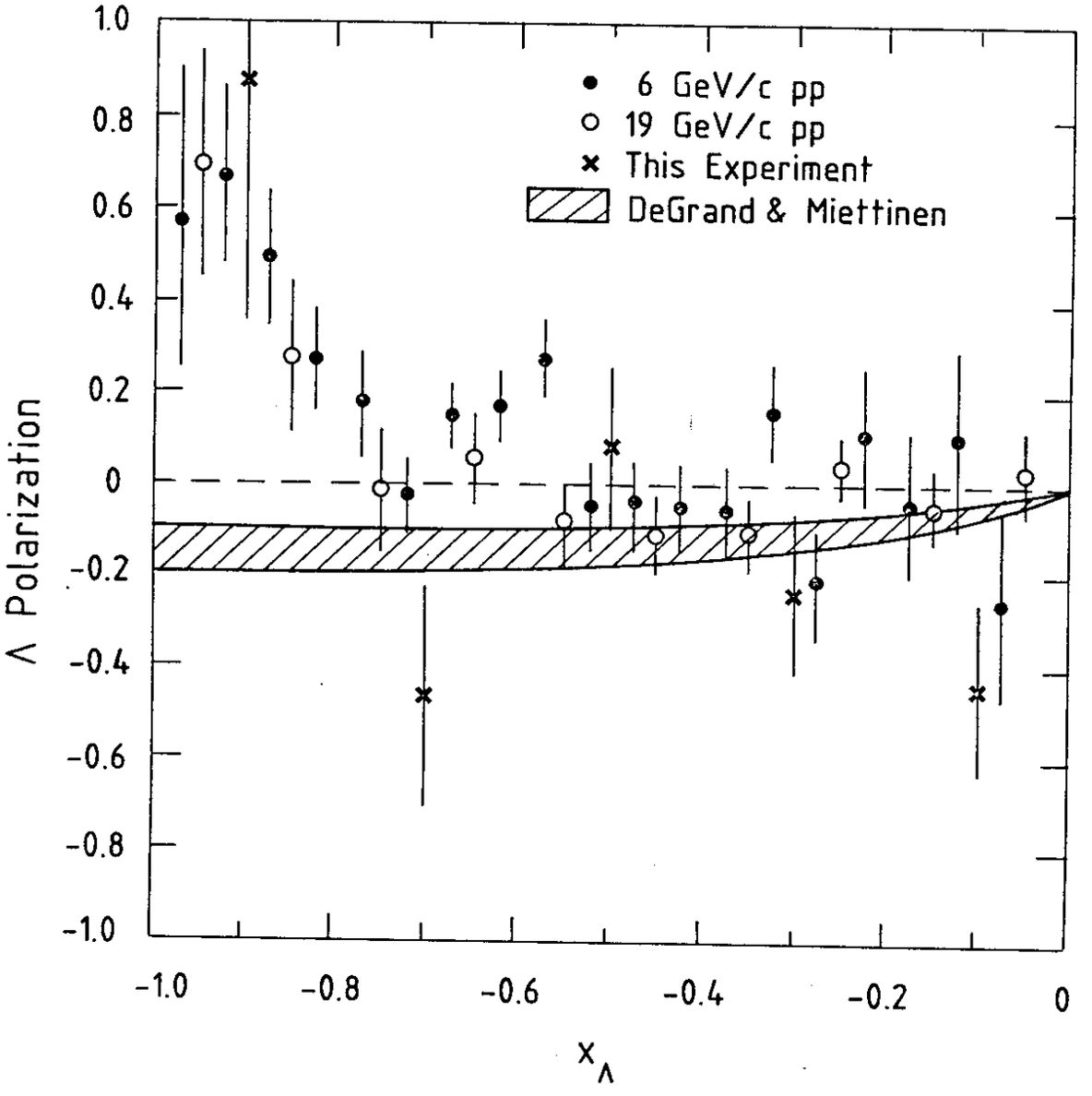
1.0
0.8
0.6
0.4
0.2
0
-0.2
-0.4
-0.6
-0.8
-1.0
Λ Polarization
-1.0
-0.8
-0.6
-0.4
-0.2
0
x_Λ
6 GeV/c pp
19 GeV/c pp
This Experiment
DeGrand & Miettinen

Fig. 14

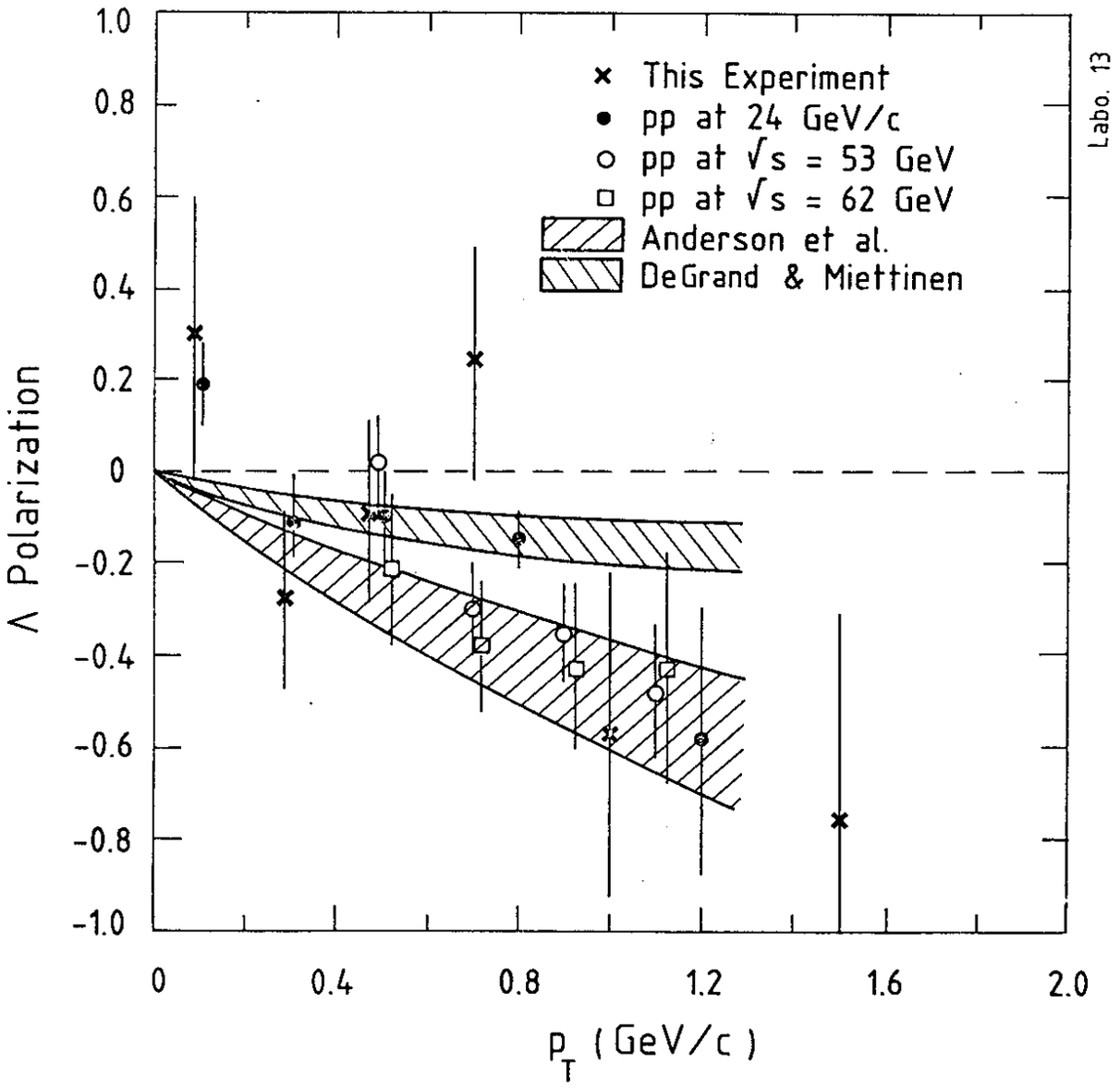
1.0
0.8
0.6
0.4
0.2
0
-0.2
-0.4
-0.6
-0.8
-1.0
Λ Polarization
0
0.4
0.8
1.2
1.6
2.0
p_T (GeV/c)
× This Experiment
● pp at 24 GeV/c
○ pp at √s = 53 GeV
□ pp at √s = 62 GeV
Anderson et al.
DeGrand & Miettinen
Labo. 13

Fig. 15